On a Possible SAR Interferometric Phase Error Associated with the Scan-On-Receive Digital Beamforming

Federica Bordoni, Gerhard Krieger
Microwaves and Radar Institute, German Aerospace Centre (DLR), Germany

Abstract

Scan-on-receive is a key digital beamforming technique for future high-resolution wide-swath synthetic aperture radar (SAR) systems. A sharp and high gain receive beam, steered towards the expected direction of arrival of the backscattering signal, allows to improve the SAR imaging performance, compared to a conventional approach. Nevertheless, it also exposes the system to new errors. A recent analysis has highlighted the relevant effect of terrain height variations and pulse duration on the SAR image radiometric quality, in view of the demanding requirements of future SAR products. This paper investigates a possible effect on the interferometric SAR performance.

1 Introduction

Scan-on-receive (SCORE) is one of the most significant digital beamforming (DBF) techniques for future high-resolution wide-swath (HRWS) spaceborne synthetic aperture radar (SAR) systems [1]. It plays a key role in the implementation of advanced missions and projects, such as the U.S.-Indian NISAR and Japanese ALOS-4 missions, the European Copernicus missions ROSE-L and Sentinel-1 Next Generation, and the highly innovative German mission proposal Tandem-L [2]-[5].

According to SCORE, a wide swath is illuminated by using a broad transmit (Tx) beam; whereas on receive (Rx), multiple digital channels are combined onboard in order to realize a sharp and high gain elevation beam, that scans the illuminated swath from near to far range, following the pulse echo as it travels along the ground range direction. Compared to a conventional technique, SCORE allows to achieve a higher signal-to-noise ratio and a more efficient suppression of the range ambiguous signals. Nevertheless, it also involves new possible sources of error, related with a mismatch between the steering direction of the SCORE Rx beam and the instantaneous direction of arrival (DoA) of the Rx signal [6], [7].

Particularly advantageous for its relatively simple and cost-effective implementation is the basic SCORE formulation, conceived for "short pulses" and considered for the realization of systems using pulses with an extension lower than the SCORE beam width [1], [8]. Here the steering direction of the Rx beam corresponds one-to-one with the range time. Accordingly, each sample received, during the pulse duration, from a given DoA is weighted by a different SCORE pattern value. Consequently, the impulse response function (IRF) of the SAR image formation process may be modulated by the SCORE Rx pattern and differ from the ideally expected amplified version of the conventional (single channel) IRF [9].

A recent analysis has shown that the SCORE pattern modulation may result in a relevant space-variant degradation of the peak power and energy of the IRF, depending on the system parameters, the SCORE steering law, and the acquisition geometry [9], [10]. Especially scenarios characterized by fast topographic variations require attention, in view of the demanding requirements on the radiometric quality of future SAR images [9], [10]. Moreover, the SCORE pattern modulation affects the phase of the IRF. In fact, depending on the system parameters and acquisition geometry, the IRF may be not real, as in the conventional case, but present a space-variant phase term [9].

The unconventional dependence of the SCORE IRF phase on the acquisition geometry open the question on a possible degradation of the interferometric SAR (InSAR) performance in SCORE-based systems. This paper provides a first answer to this important question. The problem of interest and the considered data model are explained more in detail in the next section, followed by the numerical analysis of representative acquisition scenarios.

2 Model and Problem Statement

Let us consider a spaceborne DBF SAR system with SCORE capability, operating in stripmap mode (coupled with SCORE). The architecture is based on a planar array antenna with K digital Rx elevation channels, uniformly distributed along the antenna height, h_{ant}. Without loss of generality, the array element spacing, $d = h_{ant}/K$, is assumed small enough to allow approximating the antenna elevation Rx pattern by the array factor (AF):

$$AF(\theta) = \sum_{k=1}^{K} \exp\left\{ j \frac{2\pi d (k - 0.5 - 0.5K) \sin(\theta - \theta_{tilt})}{\lambda} \right\} \approx$$

$$\approx K \operatorname{sinc}\left\{ \frac{h_{ant} \sin(\theta - \theta_{tilt})}{\lambda} \right\}, \qquad (1)$$

where θ denotes the elevation angle measured w.r.t. nadir in the zero-Doppler plane, i.e., the look angle; θ_{tilt} the antenna tilt angle; λ the radar wavelength associated with the carrier frequency (the dependence on the pulse bandwidth is neglected, for simplicity [7]).

The elevation Rx pattern is steered in real time towards the expected DoA of the Rx signal by the SCORE DBF. This is obtained by summing up the multichannel digital Rx signals, previously multiplied by a time-variant phase. In particular, the SCORE steering direction, θ_{ste}, is independent of the azimuth time, τ, and corresponds one-to-one with the range time, t, according to a simple reference topographic profile, the zero-Doppler geometry, and the expected ground position of the center of the travelling pulse [1]. It is worth to remark that, since the SCORE steering law, $\theta_{ste}(t)$, does not depend on the azimuth time, terrain height variations in the azimuth direction remain unmodelled and may result in a steering error [6], [9].

Let us neglect, for simplicity, the effect of the range cell migration on SCORE. This is justified, at least in first approximation, for typical HRWS spaceborne systems parameters [7], [9]. Based on the previous assumptions, SCORE behavior can be investigated by considering only the zero-Doppler geometry and the one-dimensional SAR processing in range. In fact, the SAR image formation process can be modelled as a linear time-varying filter, whose transfer function (TF), for a point target at (t_0, τ_0), is given by [9]:

$$H_s(f, t_0, \tau_0) = C(f)\ W_{AF}(f, t_0, \tau_0)\ W(f)\ C^*(f)\ , \quad (2)$$

where $C(f)$ denotes the discrete-time Fourier transform of the transmitted chirp pulse; $(\cdot)^*$ the complex conjugate operator; $W(f)$ a possible SAR processing Rx window, used at range compression stage to reduce the sidelobe level of the IRF; and

$$W_{AF}(f, t_0, \tau_0) = \left. w_{AF}(t, t_0, \tau_0) \right|_{t = f/K_r}, \quad (3)$$

with

$$w_{AF}(t, t_0, \tau_0) = AF\big(\theta_{ste}(t), \theta_{act}(t_0, \tau_0)\big), \quad |t - t_0| \le \frac{T}{2}, \ (4)$$

being K_r the chirp rate, T the chirp pulse duration, $AF\big(\theta_{ste}(t), \theta_{act}(t_0, \tau_0)\big)$ the antenna AF, i.e., the SCORE Rx pattern, steered towards $\theta_{ste}(t)$ and computed in the DoA of the Rx signal, $\theta_{act}(t_0, \tau_0)$.

Eq. (2) shows that SCORE DBF behaves like a window, $w_{AF}(t, t_0, \tau_0)$. In fact, each sample received from the point target with DoA, $\theta_{act}(t_0, \tau_0)$, during the pulse duration, is weighted by a different SCORE pattern value, according to the SCORE steering law, $\theta_{ste}(t)$.

Note that in the *ideal case* of a very short pulse and a steering direction matching, in t_0, the actual DoA of the target:

$$H_s(f) = K\ C(f)\ W(f)\ C^*(f)\ , \quad (5)$$

i.e., the SCORE system just amplifies by a factor K the TF of the conventional (single channel) SAR system. In a more realistic case, where the pulse duration is not negligible and

unmodelled terrain height characterizes the imaged scene, the SCORE pattern window in (4) affects both the amplitude and phase of the IRF. In particular, w.r.t. the ideal case, energy and peak power of the IRF degrades, so that a radiometric loss on the SCORE SAR image occurs. Moreover, for imaged scenes characterized by unmodelled terrain height, the SCORE pattern window may be visibly asymmetric w.r.t. t_0. As a consequence, in general, the IRF is not real as in the ideal and conventional case, but a phase occurs, which depends according to (4) on the system parameters, the SCORE steering law, and the acquisition geometry.

The effect of the SCORE pattern weighting on the radiometric properties of the SAR image is analysed in detail in [9]. In the following, the question is investigated, to what extent the phase of the SCORE IRF may affect the InSAR performance.

3   Numerical Analysis

Let us consider, as reference for the reported numerical analysis, the parameters in Tab. 1: a L-band SCORE SAR system, with a 10 m high planar antenna, orbiting at an altitude of 745 km; the pulse duration is 15 μs; the SAR processing Rx window is a Hamming window with coefficient $\alpha = 0.6$; the SCORE steering law is based on a pure spherical Earth model without terrain height.

It is worth to remark that the TF in (2) depends on the radar wavelength only through the beam width of the SCORE Rx pattern. Accordingly, as regards the SCORE behavior, the reference L-band system is equivalent, for instance, to a C-band system with $h_{ant} = 2.3$ m and $\lambda = 5.54$ cm.

As regards the imaged scene, let us first consider a single point target, located at (t_0, τ_0), with an unmodelled elevation, Δh, of 500 m, and an actual DoA, $\theta_{act}(t_0, \tau_0)$, of 27.82 deg.

The SCORE pattern sector, weighting the samples received from the target, is shown in Fig. 1. Note that the figure refers to the equivalent representation of the SCORE pattern window in (4):

$$w_{AF}(t, t_0, \tau_0) = AF\big(\theta_{act}(t_0, \tau_0), \theta_{ste}(t)\big), \quad |t - t_0| \le \frac{T}{2}, \ (6)$$

where the AF is pointed towards $\theta_{act}(t_0, \tau_0)$ and computed over the steering interval, $\left.\theta_{ste}(t)\right|_{|t - t_0| \le T/2}$. As shown in the

Quantity	Value
Orbit Height, H_{orb}	745 km
Ant. Tilt Angle, θ_{tilt}	27.93 deg
Rx Antenna Height, h_{ant}	10 m
Nr. of Digital Rx Elev. Channels, K	25
RF Center Frequency	1.2575 GHz
Chirp Duration, T	15 μs
SAR processing Rx window, W	Hamming ($\alpha = 0.6$)
SCORE steering law	@ no elevation

Table 1 Reference system parameters.

figure, the pattern sector is visibly asymmetric w.r.t. $\theta_{ste}(t_0) = 27.76$ deg, due to Δh and the related mismatch between $\theta_{act}(t_0, \tau_0)$ and $\theta_{ste}(t_0)$.

As a consequence of the asymmetric SCORE pattern weighting, the SCORE IRF (in Fig. 2) presents a non-zero phase term, antisymmetric w.r.t. the target position. More in detail, the IRF phase shows an almost linear trend over the IRF mainlobe interval, where the IRF amplitude significantly differs from zero, with a maximum value of about 1 deg. More in general, this maximum value is proportional to Δh, and slightly dependent on the SAR Rx window (slightly larger for milder sidelobe suppressions). Indeed, the SAR Rx window mainly produces a spread of the phase variation over the actual IRF mainlobe interval. Moreover, a larger sidelobe suppression increases, in general, the linearity of the phase over this interval.

As regards the interferometric phase, the phase difference between SCORE IRFs does not differ from the conventional one, as long as the SCORE pattern window is the same for the combined SCORE IRFs. This condition, however, may not be verified for relevant InSAR geometries, such as multi-pass acquisitions characterized by residual pointing errors or single-pass bistatic acquisitions.

Fig. 3 considers the effect of a possible tilt error. It shows the phase difference (i.e., the interferometric phase error associated with SCORE DBF) between the IRF in Fig. 2 and a second IRF, obtained by assuming the same parameters except for an unknown antenna tilt offset, $\Delta\theta_{tilt}$, of 0.005 deg and ±0.01 deg. The unknown tilt error translates directly into a shift of the steering interval, $\theta_{ste}(t)|_{|t-t_0| \leq T/2}$, and a slightly different SCORE pattern weighting, producing the phase difference in Fig. 3. As shown in the figure, for the considered case, the interferometric phase error varies between plus and minus 0.1 - 0.2 deg over the interval, where the amplitude of the IRF (Fig. 2) significantly differs from zero. More in general, the obtained results show that the maximum value of the phase difference is directly proportional to $\Delta\theta_{tilt}$, but independent of Δh.

Moreover, slightly larger phase errors occur for sharper beams, longer pulses, milder IRF sidelobe attenuations, and moving from the far to the near range.

Fig. 4 refers to a distributed target scenario: the SAR system parameters are those in Tab. 1, but a homogeneously backscattering surface is assumed, with a constant unmodelled terrain height of 500 m. The SCORE SAR image is simulated by considering the SAR processing steps in (2). The figure illustrates the residual phase difference, between two corresponding range lines of the simulated SCORE SAR images, for a tilt error of 0.005 and 0.01 deg. The effect of the SAR Rx window is also investigated by considering a Hamming ($\alpha = 0.6$) and a rectangular window. The obtained interferometric phase error resembles an unbias stationary random process. When a Hamming SAR Rx window is considered, the error has a standard deviation (std) around 0.1 and 0.2 deg, respectively for the considered tilt offsets. Actually, the obtained results
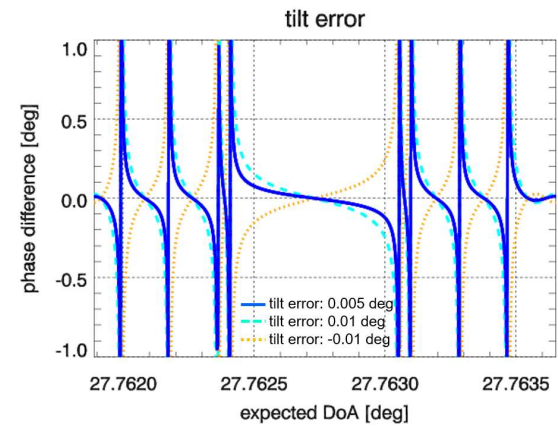
suggest that the phase error for the distributed scene (Fig. 4) can be derived from the analysis of the IRF (Fig. 3). In
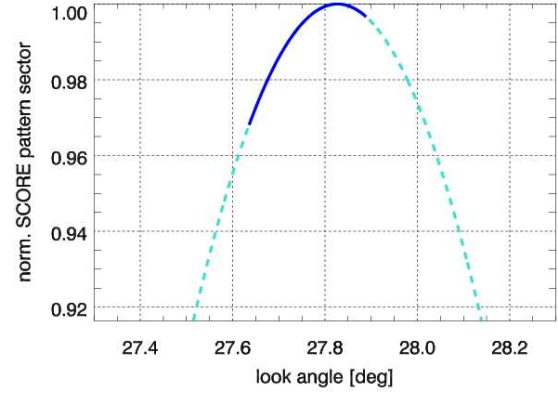

Figure 1 Point target: normalized SCORE pattern sector (solid line) weighting the Rx samples. [Δh: 500 m; θ_{act}: 27.82 deg; $\theta_{ste}(t_0) = 27.76$ deg.]
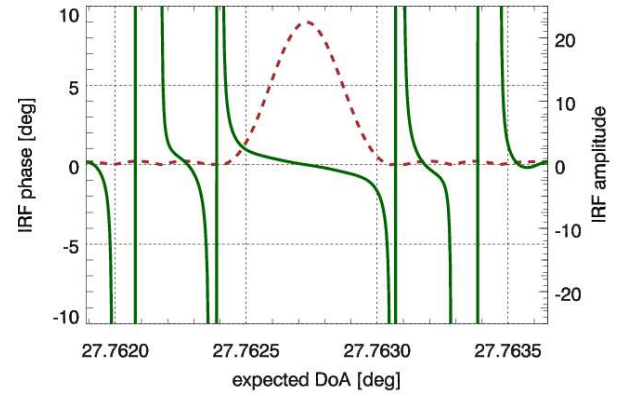
Figure 2 Point target: amplitude and phase of the IRF. [Δh: 500 m; θ_{act}: 27.82 deg; $\theta_{ste}(t_0) = 27.76$ deg; SAR Rx window: Hamming ($\alpha = 0.6$).]

Figure 3 Point target: phase difference between two IRFs, associated with SCORE DBF, for different tilt errors. [Δh: 500 m; θ_{act}: 27.82 deg; $\theta_{ste}(t_0) = 27.76$ deg; SAR Rx window: Hamming ($\alpha = 0.6$).]
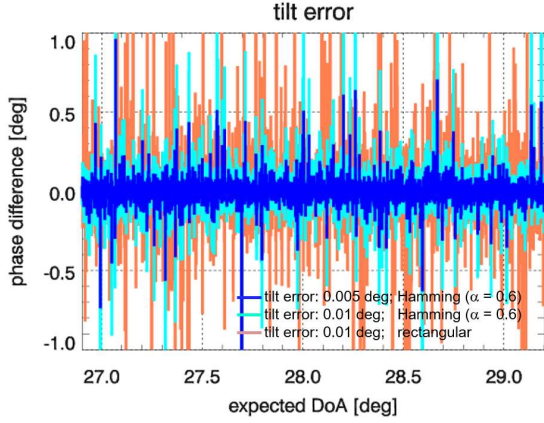
Figure 4 Distributed uniform target: phase difference between two corresponding range lines of the simulated SAR images, for different tilt errors and SAR Rx windows.

fact, the mentioned std reflects the maximum residual phase variation, occurring in correspondence of the mainlobe of the IRF. When a rectangular SAR Rx window is applied, the std increases by a factor of about 2, due to the unsuppressed phase components associated with the sidelobes of the IRF.

Figs. 5-6 refer to a bistatic geometry for single-pass cross-track InSAR: two identical SAR systems (as in Tab. 1), with the same azimuth position, flying at the same altitude on parallel tracks, and separated by a perpendicular baseline of 10 km. The imaged scene and acquisition geometry of the first satellite is the same considered in the previous analysis, i.e., a point target with θ_{act} = 27.82 deg and Δh = 500 m. At the second satellite (closer to the target), the actual DoA is 27.24 deg. Any source of pointing errors is here neglected.

Fig. 5 shows the SCORE pattern sectors weighting the samples received by the two InSAR systems. They differ from each other because of the spatial separation of the two platforms and the dependence on the slant range of both the angular mismatch, $\theta_{act}(t_0, \tau_0) - \theta_{ste}(t_0)$, and the SCORE steering velocity. In particular, for larger look angles, the steering velocity decreases and the angular extension of the pattern sectors reduces.

Fig. 6 shows the phase difference between the (coregistered) IRFs of the two satellites, associated with SCORE DBF (other phase contributes are not considered): the measured interferometric phase error, associated with SCORE DBF, varies between about plus and minus 0.1 deg over the relevant interval, and is comparable with that shown in Fig. 3 for a tilt error of 0.005 deg. In this case too, the error slightly increases moving towards the near range, for sharper SCORE beams, and for longer pulses. Nevertheless, differently from the interferometric phase error in Fig. 3, the error in Fig. 6 does depend on the unmodelled target elevation, Δh. In particular, for Δh = 0, both the IRFs would (approximately) have a zero phase, and no interferometric phase error would occur; on the other hand, in the

limiting case of Δh = 4000 m the error would be nearly 10 times larger than that in Fig. 6.

The previous results provide a first indication on the magnitude of the InSAR phase spurious component that may occur in SCORE-based acquisitions. Let us now shortly discuss the impact of this phase error on the measurement of physical quantities of interest associated with the InSAR phase. As regards the phase error associated with a mispointing, let us consider a differential InSAR measurement, based on multi-pass acquisitions: here an error, $\Delta\phi$, of 0.2 deg, would translate into a line-of-sight displacement error, $\Delta r = \lambda \Delta\phi / 4\pi$, below 0.01 mm and 0.1 mm for radar wavelength, λ, of about 3 cm and 24 cm, respectively. As regards the phase error associated with a bistatic acquisition, let us consider an across-track InSAR measurement: here a phase error of 1 deg would translate into an elevation error of about 1/360 of the assumed height of ambiguity.
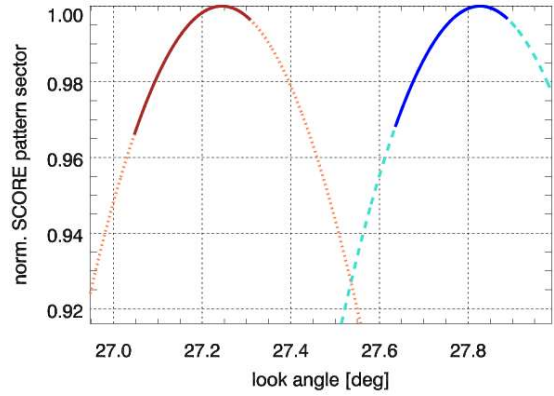
Figure 5 Point target: normalized SCORE pattern sector (solid line) weighting the samples received by two InSAR systems. [Δh: 500 m; θ_{act}: 27.24 and 27.82 deg; $\theta_{ste}(t_0)$: 27.18 deg and 27.76 deg; perpendicular baseline: 10 km.]
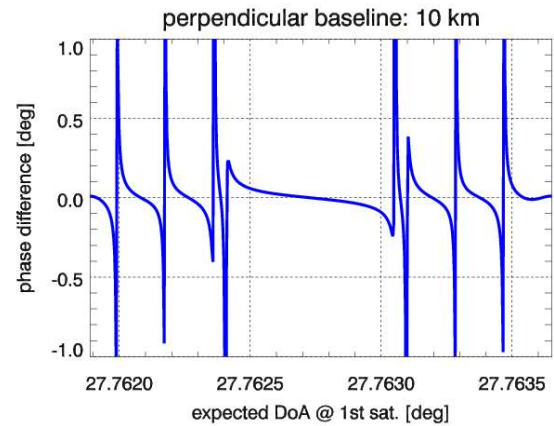
Figure 6 Point target: phase difference associated with SCORE DBF between IRFs acquired by two InSAR systems. [Δh: 500 m; θ_{act}: 27.18 and 27.82 deg; SAR Rx window: Hamming (α = 0.6); perpendicular baseline: 10 km.]

Conclusion

The SCORE DBF may introduce a spurious term on the InSAR phase extracted from SAR images acquired under different geometric conditions. This paper provides a first analysis of the phase error that may occur in presence of a pointing error or a large spatial separation between the InSAR platforms.

The obtained results indicate that the InSAR phase error due to a mispointing is proportional to the pointing offset, and is independent of the imaged surface elevation. Whereas the error associated with a bistatic acquisition is proportional to a possible unmodelled terrain height. The SAR Rx window, used to reduce the sidelobe level of the IRF, also plays a role, mitigating the error, compared to a rectangular window. Moreover, both kinds of errors become more severe moving from the far to the near range, for sharper SCORE beams, and longer transmitted pulses. In typical acquisitions scenarios, the InSAR phase errors associated with a mispointing or a large InSAR baseline, are expected to be below 0.2 deg or 1 deg, respectively.

References

[1] M. Suess, B. Grafmueller, R. Zahn, "A Novel High Resolution, Wide Swath SAR System", Proc. IGARSS, vol. 3, July 2001, pp. 1013-1015.

[2] P. Rosen, R. Kumar, "NASA-ISRO SAR (NISAR) Mission Status", Proc. IEEE RadarConf, Atlanta, GA, USA, 2021, pp. 1-6.

[3] S. Miura, Y. Kankaku, T. Motohka, K. Yamamoto, S. Suzuki, "ALOS-4 Current Status", in Proc. SPIE Sensors, Systems, and Next-Generation Satellites XXV, vol. 11858 1185809, SPIE Remote Sens., Online Only, Sept. 2021, pp. 1-10.

[4] D. Geudtner, N. Gebert, M. Tossaint, M. Davidson, F. Heliere, I. Navas Traver, R. Furnell, R. Torres, "Copernicus and ESA SAR Missions", Proc. IEEE RadarConf, Atlanta, GA, USA, 2021, pp. 1-6.

[5] A. Moreira, G. Krieger, I. Hajnsek, K. Papathanassiou, M. Younis, P. Lopez-Dekker, S. Huber, M. Villano, M. Pardini, "Tandem-L: A Highly Innovative Bistatic SAR Mission for Global Observation of Dynamic Processes on the Earth's Surface", IEEE Geosci. and Remote Sens. Magazine, vol. 3, no. 2, pp. 8-23, June 2015.

[6] F. Bordoni, M. Rodriguez, P. Prats, G. Krieger, "The Effect of Topography on SCORE: an Investigation Based on Simulated Spaceborne Multichannel SAR Data", Proc. EUSAR, Aachen, DE, June 2018, pp.1130-1134.

[7] F. Bordoni, M. Rodriguez, G. Krieger, "Possible Sources of Imaging Performance Degradation in Advanced Spaceborne SAR Systems Based on Scan-On-Receive", Proc. IEEE RadarConf, Sept. 2020, pp. 1-4.

[8] M. Younis, T. Rommel, F. Bordoni, G. Krieger, A. Moreira, "On the Pulse Extension Loss in Digital Beamforming SAR", IEEE Geosci. and Remote Sens. Letters, vol. 12, No. 7, pp. 1436 – 1440, Oct. 2015

[9] F. Bordoni, G. Krieger, D. Lind, "Radiometric Degradation Associated with Terrain Height Variations and Pulse Duration in Scan-On-Receive SAR Images", IEEE Tran. on Geosci. and Remote Sen., Vol. 60, Feb. 2022, pp. 1-14.

[10] F. Bordoni, D. Lind, A. Jakobsson, G. Krieger, "Unconventional Sources of Error in High-Resolution Wide-Swath SAR Systems based on Scan-On-Receive", Proc. EUSAR, Leipzig, DE, March 2021, pp. 1116-1119.